

Simulation of self-compacting steel fibre reinforced concrete using an enhanced SPH methodology

Abdulkarim Mimoun & Sivakumar Kulasegaram
School of Engineering, Cardiff University, Cardiff, UK

ABSTRACT: Accurate prediction of self-compacting fibre reinforced concrete (SCFRC) flow, passing and filling behaviour is not a trivial task, particularly in the presence of heavy reinforcement, complex formwork shapes and large size of aggregates. In this regard, complex formwork shapes and large size of aggregate can play an important role in fibre orientation and distribution during the flow of fibre reinforced self-compacting concrete and can thus significantly influence mechanical behaviour of the hardened material. Due to the nature of self-compacting concrete mix and widely varying properties of its constituents, it is hugely challenging to understand the rheological behaviour of the concrete mix. For this reason, it is necessary to thoroughly comprehend fresh property by understanding its rheology. The quality control and accurate prediction of the SCFRC rheology are crucial for the success of its production.

A three-dimensional meshless smoothed particle hydrodynamics (SPH) computational approach, treating the SCFRC mix as a non-Newtonian Bingham fluid constitutive model has been coupled with the Lagrangian momentum and continuity equations to simulate the flow. The aim of this numerical simulation is to investigate the capabilities of the SPH methodology in predicting the flow and passing ability of SCFRC mixes through gaps in reinforcing bars. To confirm that the concrete mixes flow homogeneously, the distribution and orientation of steel fibres in the mixes have been simulated and compared against observations made in the laboratory experiments. It is revealed that the simulated flow behaviour of SCFRC compares well with results obtained in the laboratory tests.

Keywords: Self-compacting steel fibre reinforced concrete, Fibre orientation and distribution, Smooth particle hydrodynamic, 3D simulation.

1 INTRODUCTION

Self-compacting steel fibre reinforced concrete (SCSFRC) may contribute to significant development of high quality complex concrete structures and open new applications for concrete. The addition of fibres makes the fresh concrete stiffer and reduces its workability. This also limits the number of fibres that can be uniformly orientated and distributed in the presence of heavy reinforcement, complex formwork shapes and large aggregates. As the orientation of fibres alter throughout the production of the concrete, it is essential to understand these changes in the fibre orientation. In particular, the orientation and distribution of fibres may be significantly affected, especially when the concrete is cast in the presence of heavy reinforcements. In the past, most of the study focused on visual inspection of fibres in hardened concrete parts cut after casting (Bernasconi et al. 2012; Lee et al. 2002; Zak et al. 2001) and the prediction of the typical orientation factor of fibres from the cut sections (Martinie & Roussel 2011).

The prediction of SCSFRC flow and its passing and filling behaviour is very challenging particularly

within the congestion of reinforced formwork geometry and in the presence of reinforcing steels. However, an understanding of the flow behaviour and its properties is important for producing high-quality SCC. The most cost-effective way to gain such an understanding is by performing computational simulations, which will enable one to fully characterize the flow behaviour of SCSFRC and to reveal the orientation of fibres inside the complex formwork shapes. The rheological behaviour of fresh concrete mix must be consistent with the formworks of complex shapes to ensure the production of complete and high-quality casting of structural elements. In this work, a three-dimensional Lagrangian smooth particle hydrodynamics (SPH) method is used to simulate and predict the flow of SCSFRC. SPH method is ideal for simulating the flow to analyze the passing ability and filling ability of SCSFRC mixes, irrespective of their characteristic compressive strength. These simulations will provide information about the distribution and orientation of fibres throughout the entire process of casting SCSFRC into the formworks of complex shapes to ensure that the mixture flows as a homogeneous mass without any sign of segregation or blockage. In this

paper, a simple method has been established to predict the distribution and orientation of steel fibres in self-compacting concrete mixes during flow-ability (Slump Flow test), pass-ability and fill-ability (L-box test) tests.

2 DEVELOPMENT OF THE SELF COMPACTING NORMAL-STRENGTH STEEL FIBRE REINFORCED CONCRETE MIXES.

A laboratory study was conducted to produce various grades of SCSFRC mixes (with nominal 28 days cube compressive strengths of 30 MPa, 40 MPa, 50 MPa, 60 MPa and 70 MPa). The fundamental materials and secondary materials for the SCC mix are produced following the European Federation of Specialist Construction Chemicals and Concrete Systems (EFNARC) guidelines (EFNARC 2005). These mixes were developed using a mix design method for SCC based on the desired target plastic-viscosity and compressive strength in accordance with mix design method proposed by Abo Dhaheer et al. (2016a, 2016b), which rationalized and simplified the method recommended previously by Karihaloo and Ghanbari (2012), Deeb and Karihaloo (2013). As an example, the amounts and specifications of the components used in the SCC design mix with target compressive strength 40MPa are shown in Table 1. Portland limestone cement (PLC) (CEM II/A-L/32.5R) conforming to (BS EN 197-1 2011) with a specific gravity of 2.95 and Ground granulated blast-furnace slag (GGBS) with a specific gravity of 2.40 were used as the main cement and cement replacement materials respectively. A new generation of polycarboxylic

Table 1. Constituents and proportions for SCSFRC mixes (kg/m³).

Mix strength grade 40 MPa	
Cement: kg/m ³	270
GGBS*: kg/m ³	90
Cementitious materials (cement + GGBS): kg/m ³	360
Water: kg/m ³	205
Superplasticiser: kg/m ³	2.3
Water/cementitious materials ratio	0.57
Superplasticiser/cementitious materials ratio	0.64
Limestone powder: kg/m ³	143
steel fibre volume (SF) (0.5%): kg/m ³	40
Fine aggregate (<2 mm)**	740
FA ^a : kg/m ³	240
FA ^b : kg/m ³	500
Coarse aggregate: kg/m ³ (size of 10 mm)	839
t ₅₀₀ in flow: s	1.40
Slump Flow spread : mm	600
Plastic viscosity (PV): Pa. S	27

*Ground granulated blast-furnace slag.

**Fine aggregate <2 mm (Note: a part of the fine aggregate is the coarser fraction of the limestone powder, FA^a 125 µm–2 mm, whereas FA^b refers to natural river sand < 2 mm).

ether-based superplasticiser (SP) with specific gravity of 1.07 was used in all the test mixes. Crushed limestone coarse aggregate with maximum particle size of 20 mm and a specific gravity of 2.80 was used, while the fine aggregate was river sand (less than 2 mm) having a specific gravity of 2.65. Limestone powder (LP) as a filler with maximum particle size of 125 µm (specific gravity 2.40) was used. A part of the river sand was substituted by an equal amount of the coarser fraction of LP in the size range 125 µm – 2 mm. All mixes were tested in the fresh state utilizing slump flow and L-box tests. The plastic viscosity of each mix was calculated using the micro-mechanical procedure described by (Ghanbari & Karihaloo 2009).

3 MODELLING THE FLOW-ABILITY, PASSING-ABILITY AND FILLING-ABILITY OF STEEL FIBRE SUSPENDED SELF-COMPACTING CONCRETE BASED ON EXPERIMENT

In the rheological studies to characterize fresh concrete, SCSFRC is understood as a suspension of solid particles (coarse aggregate and steel fibre) in a fluid phase (cement paste), in which various of particle size distribution and fluid stage are typically enhanced to meet the three main properties of SCSFRC in the fresh state: filling ability, passing ability, and segregation resistance.

SCSFRC mixes are designed to meet flowability and cohesiveness (i.e., resistance to segregation) standards utilizing the slump cone test. In this test, the time for the SCSFRC mix to spread to a diameter of 500 mm (T₅₀₀) after the cone filled with the mix has been suddenly lifted is recorded, as well as the diameter of the spread when the flow stops (EFNARC 2005). The resistance to segregation and blockage is checked visually between the coarse aggregate and steel fibre (Figure 1).

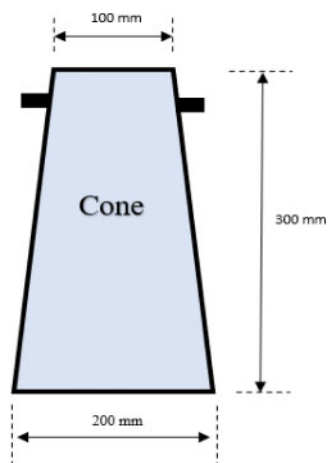


Figure 1. Dimension of Flow test of SCSFRC.

To test the ability of a SCSFRC mix to pass and fill the formwork containing reinforcement under its own weight, the L-box apparatus is used (EFNARC 2005). The vertical leg of the L-box is initially filled with the SCSFRC mix. At the bottom of this leg is a gate with two or three rods in front of it. When the gate is lifted, the mix flows into the horizontal part of the L-box through the gaps between the rods. The times for the mix to reach 200 mm (T_{200}) and 400 mm (T_{400}) from the gate are recorded, as well as the time it takes the mix to level off in the horizontal leg of the L-box. Again, it is required that no coarse large aggregate particles or steel fibres be blocked by the rods (Figure 2).

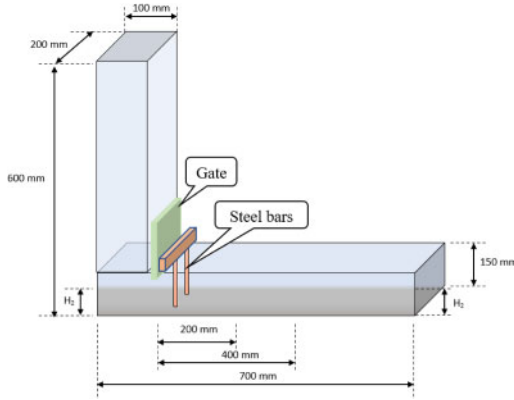


Figure 2. Dimension of L-box test of SCSFRC.

The addition of steel fibres enhances the mechanical characteristics and the ductility of SCC in much the same approach as in vibrated concrete (VC). Nevertheless, the fibres significantly impair the workability of SCC due to their elongated shape and large surface area. The volume of fibre added to a SCC mixture is therefore limited and depends on the fibre type used and the composition of the SCC mix. Therefore, the maximum volume of fibres is decided in such a way to manage the workability, whilst maintaining excellent flowing and passing ability. For the optimum results, the fibres require to be homogeneously distributed in the mixture without clustering or segregation and blockage.

4 MODELLING SIMULATION THE FLOW-ABILITY, PASSING-ABILITY AND FILLING-ABILITY OF SCSFRC

Since fresh SCSFRC flow in slump and L-box test configurations is a gravitational flow with large deformations, a three-dimensional smooth particle hydrodynamic (SPH) mesh-less numerical methodology is chosen here to simulate the fresh state. This section briefly introduces the fundamental governing equations, numerical model and the boundary conditions required for modelling SCSFRC flow in slump flow and L-box of tests with 3D-Lagrangian SPH method.

4.1 Governing equations

Fresh SCSFRC mix is a non-Newtonian incompressible fluid which can be described by a bilinear Bingham-type model with relation between the shear stress and shear strain rate which includes two material parameters: the yield stress (τ_y) (Badry et al. 2014) and the plastic viscosity (η) (Ghanbari & Karihaloo 2009) (Papanastasiou 1987).

$$\tau = \eta \dot{\gamma} + \tau_y (1 - e^{-m\dot{\gamma}}) \quad (1)$$

Where m is a very large number (e.g., $m = 100$). There are two basic equations to be solved in the SPH method, together with the constitutive relation – the incompressible mass and momentum conservation equations.

$$\frac{1}{\rho} \frac{D\rho}{Dt} + \nabla \cdot \mathbf{v} = 0 \quad (2)$$

To include the effect of immersed boundary, the momentum conservation equation is modified:

$$\frac{D\mathbf{v}}{Dt} = -\frac{1}{\rho} \nabla P + \frac{1}{\rho} \nabla \cdot \boldsymbol{\tau} + \mathbf{g} + \mathbf{f} \quad (3)$$

where ρ , t , \mathbf{v} , P , \mathbf{g} and $\boldsymbol{\tau}$ represent the fluid particle density, time, particle velocity, pressure, gravitational acceleration, and shear stress tensor, respectively. Here, \mathbf{f} represents the effective reaction force of the fibres on the fluid at any chosen location. However, the reaction force \mathbf{f} will not be acting on the fluid particles which do not fall within the radius of influence (or smoothing length) of any boundary particles of a given fibre. In the proposed numerical procedure, fibres are described by immersed boundaries.

4.2 Numerical implementation

A projection method based on the predictor–corrector time stepping scheme was adopted to track the Lagrangian non-Newtonian flow. The prediction step is an explicit integration in time without enforcing incompressibility. Only the viscous stress and gravity terms are considered in the momentum equation (Equation 3) and an intermediate particle velocity is obtained as:

$$\mathbf{v}_{n+1}^* = \mathbf{v}_n + \left(\mathbf{g} + \mathbf{f} + \frac{1}{\rho} \nabla \cdot \boldsymbol{\tau} \right) \Delta t \quad (4)$$

in which \mathbf{v}_n and \mathbf{v}_{n+1}^* are the particle velocity and intermediate particle velocity at time t_n and t_{n+1} , respectively. Then the correction step is performed by considering the pressure term in Equation 3

$$\frac{\mathbf{v}_{n+1} - \mathbf{v}_{n+1}^*}{\Delta t} = - \left(\frac{1}{\rho} \nabla P_{n+1} \right) \quad (5)$$

Rearranging Equation 5 gives

$$\mathbf{v}_{n+1} - \mathbf{v}_{n+1}^* = - \left(\frac{1}{\rho} \nabla P_{n+1} \right) \Delta t \quad (6)$$

where v_{n+1} is the corrected particle velocity at time step t_{n+1} . By imposing the incompressibility condition in the mass conservation equation (Equation 2), the pressure P_{n+1} in Equation 6 will be obtained. As the particle density remains constant during the flow, the velocity v_{n+1} is divergence-free so that Equation 2 can be simplified as.

$$\nabla \cdot v_{n+1} = 0 \quad (7)$$

Substitution into Equation 6 gives

$$\nabla \left(\frac{1}{\rho} \nabla P_{n+1} \right) = \frac{\nabla \cdot v_{n+1}^*}{\Delta t} \quad (8)$$

which can be rewritten as

$$\nabla^2 P_{n+1} = \frac{\rho}{\Delta t} \nabla v_{n+1}^* \quad (9)$$

where ∇^2 is the Laplacian. Solution of the second-order Poisson equation (Equation 9) gives the pressure from which the particle velocity is updated (see Equation 6). Finally, the instantaneous particle position is updated using the corrected velocity.

$$x_{n+1} = x_n + v_{n+1} \Delta t \quad (10)$$

where x_{n+1} and x_n are the particle positions at t_{n+1} and t_n , respectively.

The interaction between SPH fluid particles surrounding the rigid fibres can be modelled by treating fibres as immersed boundaries (Figure 3). This would offer a simple and efficient methodology to determine fibre orientations and distribution during the flow.

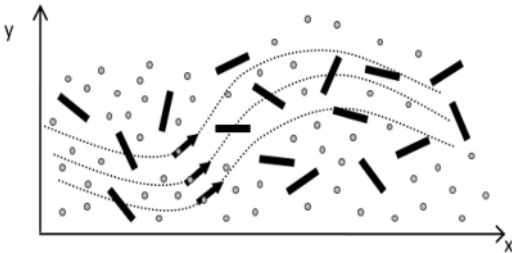


Figure 3. Schematic diagram of the flow of SCSFRC with rigid steel fibres.

5 INITIAL CONFIGURATION AND BOUNDARY CONDITION

When solving the Navier-Stokes and continuity equations, appropriate initial and boundary conditions need to be applied. Three types of boundary conditions need to be considered in the simulation of slump cone test;

a zero-pressure condition on the free surface, Dirichlet boundary condition at the wall of the cone, and Neumann conditions on the pressure gradient as illustrated in Figure 4.

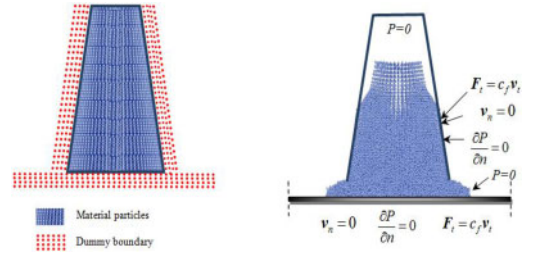


Figure 4. Slump flow and L-box test initial condition.

Four arrays of rigid dummy particles placed outside the wall of the cone were used to implement the wall boundary conditions with space r_0 between the arrays, where r_0 is the initial particle spacing. To represent the non-slip boundary conditions along the cone wall, the velocity of both the wall and dummy particles must be zero. Friction between SCC flow and boundaries was also considered and imposed on the cone wall and the bottom plate with a dynamic coefficient of friction between the SCC mix and steel equal to 0.55 Ns/m.

6 THREE-DIMENSIONAL SIMULATION RESULTS

To examine how the steel fibres will distribute and orient themselves throughout the filling process, flow (slump flow) and pass/fill (L-box) tests were conducted for SCC mix with steel fibre (Mix 40 MPa, Table 1). The steel fibres were treated as described above. The plastic viscosity (i.e. 27 Pa s) of the mix was estimated analytically using micro-mechanics based formulations. The yield stress and the dynamic coefficient of friction with the steel wall of the cone and the base plate were assumed to be 200 Pa and 0.55 Ns/m respectively.

Figure 5 illustrate the distribution of fibres and their orientation during the numerical simulation of slump flow. During the simulation of slump flow, the time for the mixtures to spread to a diameter of 500 mm ($T_{500} = 1.45$ sec) matches closely with the time measured in the laboratory (Table 2). The surface of the spread is smooth, and the fibres stay homogeneously always distributed during the flow. Similarly, the L-box tests also produced comparable results with experimental observations

The proposed method can be successfully applied in the numerical simulation of SCSFRC flow to analyze the flow, passing and filling behavior of these highly viscous fluids. The numerical results are in excellent agreement with experimental results and validate that

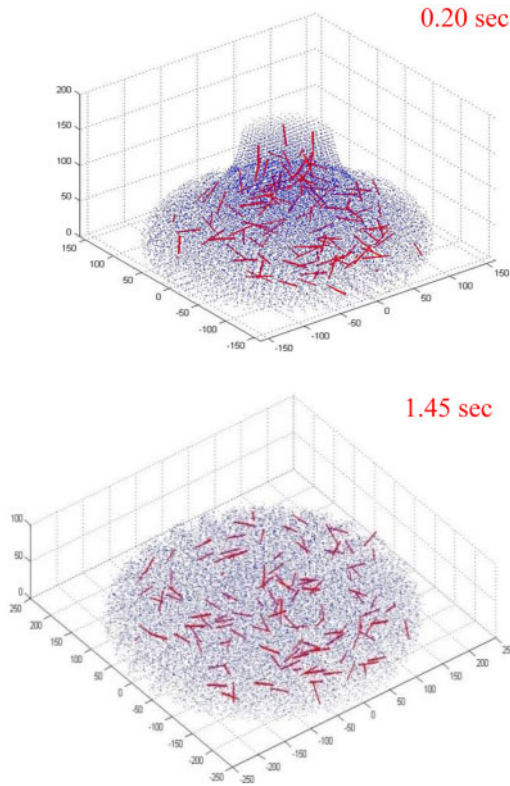


Figure 5. 3D numerical simulation of slump flow test for SCSFRC (0.5%vol fibre).

Table 2. Comparison of experimental and simulations results for slump flow and L-box tests.

	Mix strength grade: 40 MPa	
	Simulation	Experiment
t ₅₀₀ mm in Flow: s	1.45	1.40
Flow spread mm	615	600
T ₂₀₀ in L-box: s	0.90	0.93
T ₄₀₀ mm in L-box: s	1.90	1.90

the 3D SPH methodology can effectively predict the flow of fresh SCSFRC mix.

7 CONCLUSIONS

A Lagrangian SPH method has been used to simulate the flow of self-compacting normal performance concrete with steel fibre during the slump flow and L-box tests in 3-dimensional configurations. A appropriate Bingham model (Ghanbari & Karihaloo 2009)



Figure 6. Experiment of slump flow test for SCSFRC (0.5%vol fibre).

has been coupled with the Lagrangian Navier-Stokes and continuity equations to model this flow. The mixture characteristics of the SCSFRC mix have been fully incorporated implicitly through the plastic viscosity, which has been assessed exploiting the micromechanical model described in (Ghanbari & Karihaloo 2009).

The simulation of SCSFRC mixes focused on the orientations of fibres and their distributions during the flow, passing, and filling phases of the slump flow and L-box tests. The established numerical methodology is able to capture the flow, passing, and filling behaviour of SCSFRC mixes and to provide insight

into the distribution of fibres and their orientations during these phases. The comparison of the experimental and the simulation results is very encouraging. More flow simulations and validations of SCSFRC mixes (with nominal 28 days cube compressive strengths between 30 to 70 MPa) to be carried out to perform additional parametric studies and to further establish the accuracy of the numerical model.

REFERENCES

- Abo Dhaheer, M. S. *et al.* (2016a) 'Proportioning of self-compacting concrete mixes based on target plastic viscosity and compressive strength: Part II – experimental validation', *Journal of Sustainable Cement-Based Materials*. Taylor & Francis, 5(4), pp. 217–232. doi: 10.1080/21650373.2015.1036952.
- Abo Dhaheer, M. S. *et al.* (2016b) 'Proportioning of self-compacting concrete mixes based on target plastic viscosity and compressive strength: Part I – mix design procedure', *Journal of Sustainable Cement-Based Materials*. Taylor & Francis, 5(4), pp. 199–216. doi: 10.1080/21650373.2015.1039625.
- Badry, F., Kulasegaram, S. and Karihaloo, B. L. (2014) 'Estimation of the yield stress and distribution of large aggregates from slump flow test of self-compacting concrete mixes using smooth particle hydrodynamics simulation', *Journal of Sustainable Cement-Based Materials*. Taylor & Francis, 5(3), pp. 117–134. doi: 10.1080/21650373.2014.979266.
- Bernasconi, A., Cosmi, F. and Hine, P. J. (2012) 'Analysis of fibre orientation distribution in short fibre reinforced polymers: A comparison between optical and tomographic methods', *Composites Science and Technology*. Elsevier Ltd, 72(16), pp. 2002–2008. doi: 10.1016/j.compscitech.2012.08.018.
- BS EN 197-1 (2011) 'Cement?: Composition, specifications and conformity criteria for common cements', *BSI*.
- Deeb, R. and Karihaloo, B. L. (2013) 'Mix proportioning of self-compacting normal and high-strength concretes', *Magazine of Concrete Research*, 65(9), pp. 546–556. doi: 10.1680/mac.12.00164.
- EFNARC (2005) 'The European guidelines for self-compacting concrete—specification, production and use.', *The European Guidelines for Self Compacting Concrete*, (May).
- Ghanbari, A. and Karihaloo, B. L. (2009) 'Prediction of the plastic viscosity of self-compacting steel fibre reinforced concrete', *Cement and Concrete Research*. Elsevier Ltd, 39(12), pp. 1209–1216. doi: 10.1016/j.cemconres.2009.08.018.
- Karihaloo, B. L. and Ghanbari, A. (2012) 'Mix proportioning of self-compacting high-and ultrahigh-performance concretes with and without steel fibres', *Magazine of Concrete Research*, 64(12), pp. 1089–1100. doi: 10.1680/mac.11.00190.
- Lee, Y. H. *et al.* (2002) 'Characterization of fiber orientation in short fiber reinforced composites with an image processing technique', *Materials Research Innovations*, 6(2), pp. 65–72. doi: 10.1007/s10019-002-0180-8.
- Martinie, L. and Roussel, N. (2011) 'Simple tools for fiber orientation prediction in industrial practice', *Cement and Concrete Research*. Elsevier Ltd, 41(10), pp. 993–1000. doi: 10.1016/j.cemconres.2011.05.008.
- Papanastasiou, T. (1987) 'Flows of Materials with Yield', *Journal of Rheology*, 31(5), pp. 385–404. doi: 10.1122/1.549926.
- Zak, G., Park, C. B. and Benhabib, B. (2001) 'Estimation of three-dimensional fibre-orientation distribution in short-fibre composites by a two-section method', *Journal of Composite Materials*, 35(4), pp. 316–339. doi: 10.1106/65LQ-1UK7-WJ9H-K2FH.